

# Simulation Study of Photon-to-Digital Converter (PDC) Timing Specifications for LoLX Experiment

Nguyen V. H. Viet, *Member, IEEE*, Alaa Al Masri, Masaharu Nomachi, *Senior Member, IEEE*, Marc-André Tétrault, *Member, IEEE*, Soud Al Kharusi, Thomas Brunner, Christopher Chambers, Bindiya Chana, Austin de St. Croix, Eamon Egan, Marco Francesconi, David Gallacher, Luca Galli, Pietro Giampa, Damian Goeldi, Jesse Lefebvre, Chloe Malbrunot, Peter Margetak, Juliette Martin, Thomas McElroy, Mayur Patel, Bernadette Rebeiro, Fabrice Retière, El Mehdi Rtimi, Lisa Rudolph, Simon Viel, Liang Xie

**Abstract**—The Light only Liquid Xenon (LoLX) experiment is a prototype detector aimed to study liquid xenon (LXe) light properties and various photodetection technologies. LoLX is also aimed to quantify LXe’s time resolution as a potential scintillator for 10 ps time-of-flight (TOF) PET. Another key goal of LoLX is to perform a time-based separation of Cerenkov and scintillation photons for new background rejection methods in LXe experiments. To achieve this separation, LoLX is set to be equipped with photon-to-digital converters (PDCs), a photosensor type that provides a timestamp for each observed photon. To guide the PDC design, we explore requirements for time-based Cerenkov separation. We use a PDC simulator, whose input is the light information from the Geant4-based LoLX simulation model, and evaluate the separation quality against time-to-digital converter (TDC) parameters.

Simulation results with TDC parameters offer possible configurations supporting a good separation. Compared with the current filter-based approach, simulations show Cerenkov separation level increases from 54% to 71% when using PDC and time-based separation. With the current photon time profile of LoLX simulation, the results also show 71% separation is achievable with just 4 TDCs per PDC. These simulation results will lead to a specification guide for the PDC as well as expected results to compare against future PDC-based experimental measurements. In the longer term, the overall LoLX results will assist large LXe-based experiments and motivate the assembly of a LXe-based TOF-PET demonstrator system.

**Index Terms**—liquid xenon, Cerenkov radiation, photon-to-digital converter, silicon photomultiplier, time-to-digital converter

## I. INTRODUCTION

Manuscript received ... This research was undertaken thanks in part to funding from the Canada First Research Excellence Fund through the Arthur B. McDonald Astroparticle Physics Research Institute, with support from the National Sciences and Research Council of Canada (NSERC), and the Fonds de Recherche du Québec Nature et Technologies (FQRNT). This was also supported by CHELN and CHELNX projects funded by Grant INFN n. 19593, and the PQBA program of Osaka University.

N. V. H. Viet and M. Nomachi are with the Research Center for Nuclear Physics (RCNP), Osaka University, Osaka, Japan.

A. Al Masri, M.-A. Tétrault, J. Lefebvre, and E. M. Rtimi are with the Department of Electrical and Computer Engineering, Université de Sherbrooke, Sherbrooke, QC, Canada. (e-mail: Alaa.Al.Masri@USherbrooke.ca)

S. Al Kharusi, T. Brunner, C. Chambers, E. Egan, D. Gallacher, T. McElroy, B. Rebeiro, and L. Rudolph are with the Physics Department, McGill University, Montréal, QC, Canada.

B. Chana, D. Goeldi, and S. Viel are with the Department of Physics, Carleton University, Ottawa, ON, Canada.

A. de St. Croix, C. Malbrunot, P. Margetak, J. Martin, M. Patel, F. Retière, and L. Xie are with TRIUMF, Vancouver, BC, Canada.

M. Francesconi and L. Galli are with INFN, Pisa, Italy.

P. Giampa is with SNOLAB, Lively, ON, Canada.

**S**CINTILLATORS are core components for many particle physics detectors. The choice of scintillator relies on its material properties and the sought-after experimental data, generally position, deposited energy and occurrence time. Liquid xenon (LXe) is a scintillator offering attractive performances on these three figures of merit due to its good light yield, fast timing, and dual light/charge readout paths. Although it needs to be cooled to  $-110\text{ }^{\circ}\text{C}$ , and thus requires a cryostat to operate, it can be shaped to a large, continuous volume, an attractive feature for neutrino experiments like nEXO [1], which requires 1% energy resolution at 2.5 MeV Q-value of Xe-136 in its search for neutrinoless double beta decay ( $0\nu\beta\beta$ ). The Light only Liquid Xenon (LoLX) experiment [2] supports nEXO in testing candidate photosensor technologies and studying LXe light properties to achieve this goal. Then in a future phase of the experiment, LoLX will aim to achieve time-based Cerenkov-scintillation separation to explore new background rejection methods in LXe-based  $0\nu\beta\beta$  experiments [3]. Moreover, Cerenkov photons in LXe can potentially increase prompt photon statistics for fast timing applications such as time-of-flight (TOF) PET [4]. For this application, LoLX’s goal is to confirm if a 10 ps time resolution can be obtained in LXe to pave the way for PET scanners with cutting edge performance [5].

To achieve those goals, current SiPMs installed in LoLX are expected to be replaced by Photon-to-Digital Converters (PDCs), also known as digital single-photon avalanche diode (SPAD) arrays or digital SiPMs [6]. PDCs highlights are their abilities to offer sub-100 ps timing for each observed photon and to address the intrinsic timing skew limitation of large area SiPMs [7].

In this study, we used the light output information from our LoLX simulation model and redirected it to a PDC simulator, the digital SPAD array simulator (DSAS) [8]. We then explored the design parameter space, defining PDC specifications that enable the time-based Cerenkov-scintillation separation on an event-by-event basis. This study will provide specification margins for the on-going development of LoLX PDCs.

## II. SETUPS & METHODS

### A. LoLX and its Simulation Model

The LoLX Gen1 design uses a 3D printed octagon cylindrical case, enclosing an approx.  $30\text{ cm}^3$  volume (Fig. 1). This case is equipped with 24 Hamamatsu VUV4 Quad modules [9], 4 SiPMs each, so 96 SiPMs in total. To separate Cerenkov

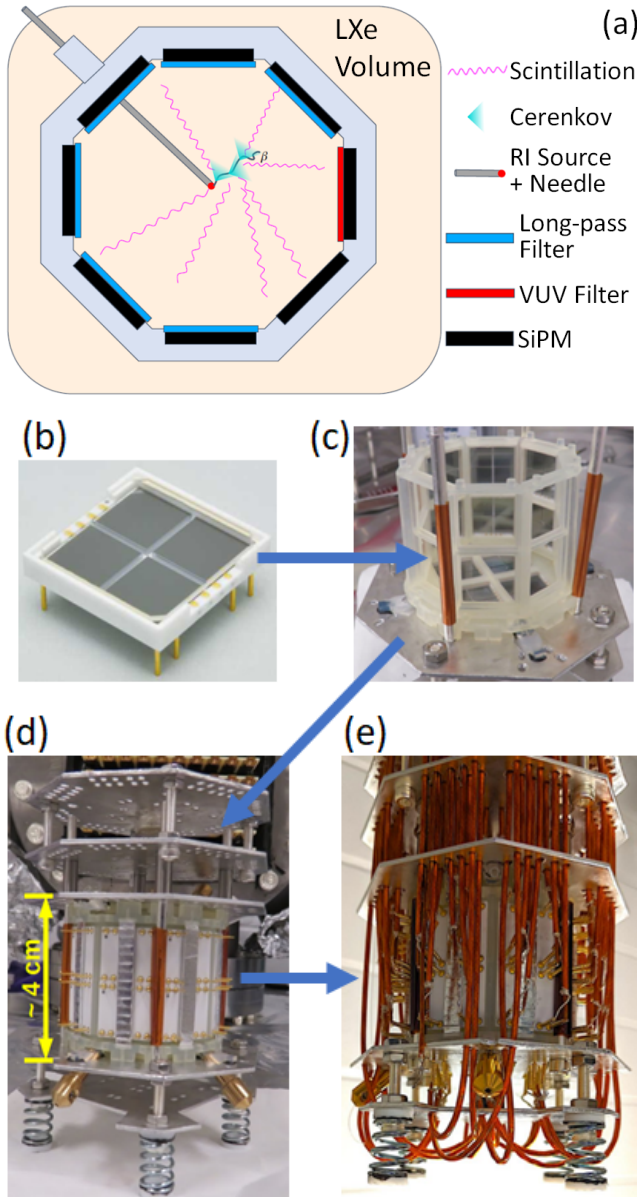


Fig. 1. (a) Sketch of LoLX Gen1 setup; (b)  $1.5\text{ cm} \times 1.5\text{ cm}$  VUV4 SiPM module; (c) 3D printed case for 24 modules; (d) assembled LoLX Gen1 detector (unwired); (e) assembled LoLX Gen1 detector (wired).

and scintillation, LoLX applies optical filters to the surface of the SiPM modules: 22 modules with long-pass filters (allow wavelength  $> 225\text{ nm}$ , mainly Cerenkov), 1 module with VUV filter (allow wavelength  $150\text{--}180\text{ nm}$ , mainly scintillation), and 1 module with no filter (bare). A Sr-90 source is inserted within the instrumented volume using a needle penetrating through the case.

LoLX simulation model was developed using Geant4 [10]. The LXe scintillation yield was set to  $46,300\text{ photons/MeV}$  while the wavelength-dependent refractive index of LXe, main factor for Cerenkov yield, was obtained from literature [11].

### B. PDC Simulator (DSAS) Setup

In this study, we recorded the photon information provided by our Geant4 model at the surfaces of the photosensors

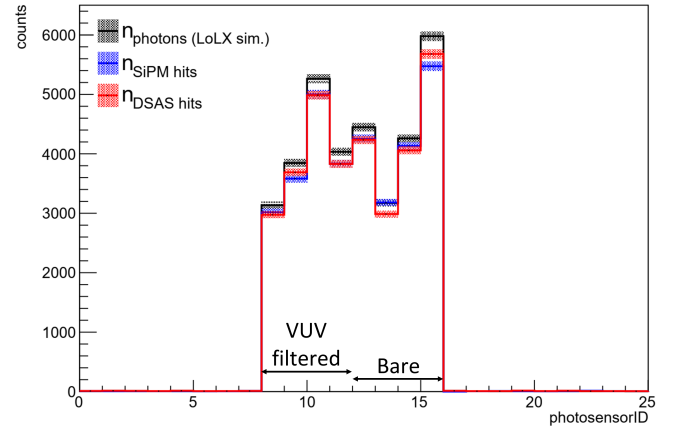


Fig. 2. Validation of the numbers of hits created by DSAS against those created by LoLX SiPM model (focus on VUV filtered and bare photosensors). In this LoLX simulation, from 200 primary  $\beta$  events, approx. 35,000 photons reach 96 sensors. The shaded bands indicate the errors as the square root of the counts for each sensor.

and passed it on the PDC simulator, DSAS. This allowed us to compare the performance of various PDC configurations using the same photon simulation baseline. The initial PDC geometry specifications in DSAS were based on LoLX's SiPMs:  $6\text{ mm} \times 6\text{ mm}$  active area,  $50\text{ }\mu\text{m}$  pitch.

Before proceeding with PDC timing study, we validated DSAS against the original Geant4 SiPM model. In Fig. 2, we compared the number of hits created by DSAS and by the SiPM model using in both the same input photon information given by the LoLX simulation. The parameter requirements for after-pulse (AP), dark count (DC), optical crosstalk (XT), and photodetection efficiency (PDE) differ between DSAS and the SiPM model. We adjusted these input parameters in DSAS to align the numbers of hits with those created by the SiPM model.

### C. PDC Timing Specification Study

This study focuses on how time-to-digital converter (TDC) jitter, least significant bit (LSB), and SPAD:TDC sharing ratio affect the separation quality. We scanned various combinations of the 3 quantities, and for each setting, we applied a time-based cut in order to maximize the number of Cerenkov photons ( $n_{\text{Ceren}}$ ) obtained while minimizing the number of scintillation photons ( $n_{\text{Scint}}$ ) remaining in the cut. The separation quality was first evaluated with both TDC jitter and LSB varied between 1 and 50 ps. The initial SPAD:TDC ratio was set to 1:1, and was subsequently altered after finding optimal jitter and LSB values. The Sr-90 ( $\beta$ ) source position was set to the center of the LXe case in this PDC timing study.

For the time-based separation purpose, the photon information input to DSAS was taken from a modification setup of LoLX Gen1 simulation model, in which no filter was applied. In the early time window, the first few nanoseconds, the photon density is significantly higher than DC and AP. Thus, DC, AP, and also XT values in DSAS were set to 0. The PDE was simply set at ideal 100%.

For comparison, in the filter-based approach, the filter setup of LoLX simulation model was also modified, in which long-

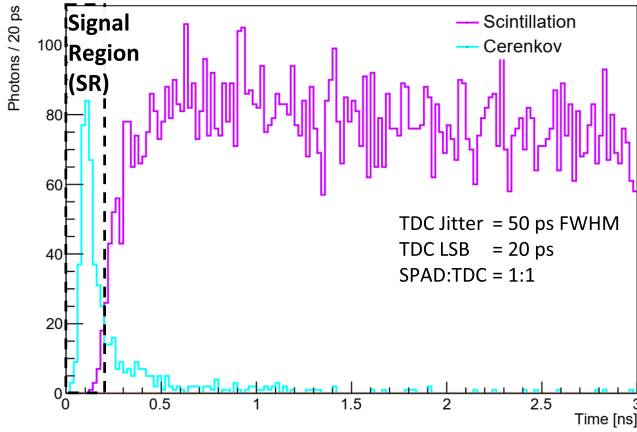


Fig. 3. Photon time profile of a bare photosensor using DSAS with focus on the early time segment. In LoLX simulation, from 5000 primary  $\beta$  events, approx. 500 Cerenkov and 140,000 scintillation photons reach this bare sensor. The signal region in this figure should be chosen to maximize the  $n_{\text{Ceren}}$  and minimize the  $n_{\text{Scint}}$  within it.

pass filters were applied to all 96 SiPMs. To ensure equivalent DC, AP, XT, and PDE values as in DSAS, the number of hits created is considered as the number of photons going through the filters and reaching the SiPM surfaces.

In the simulated filter-based approach, on average, 54% of the total Cerenkov photons go through the long-pass filters and reach the SiPM surfaces. The ratio of the  $n_{\text{Scint}}$  leaking through these filters to the  $n_{\text{Ceren}}$  going through is approx. 0.09.

Thus, the time-based cut conditions are set as:

$$f_{\text{Ceren}} \geq 55\% \quad \& \quad r_{\text{SC}} < 0.02 \quad (*)$$

in which:

$$f_{\text{Ceren}} = \frac{n_{\text{Ceren}} \text{ in SR}}{\text{Total } n_{\text{Ceren}}} \quad \& \quad r_{\text{SC}} = \frac{n_{\text{Scint}} \text{ remains in SR}}{n_{\text{Ceren}} \text{ in SR}}$$

with SR is the signal region as shown in Fig. 3. While the  $n_{\text{Ceren}}$  in this figure is much less than the  $n_{\text{Scint}}$ , it is possible to separate Cerenkov photons due to their prompt arrival.

### III. RESULTS & DISCUSSIONS

#### A. TDC Jitter & LSB

Fig. 4 shows the Cerenkov separation (as  $f_{\text{Ceren}}$ ) of 96 photosensors vs. different TDC specifications using the optimal cut position of each photosensor. For jitter  $\geq 20$  ps & LSB = 50 ps, the min  $f_{\text{Ceren}}$  is 0, meaning no cut position allows an efficient separation at some sensors. For LSB  $\leq 20$  ps, results are nearly identical, medians of 71–75%, min values of 60–63%, and max values of 81–82%, for 96 sensors.

These results indicate a good performance of the time-based separation. For most sensors, the min  $f_{\text{Ceren}}$  of the time-based separation is still better than the average 54% of Cerenkov photons reaching the sensors in the filter-based approach. Results also indicate an upper limit when going for smaller jitter and LSB, implying a similarity to raw photon data from LoLX simulation. Regarding PDC design, these results suggest minor effects of both jitter and LSB on the separation when LSB  $\leq 20$  ps.

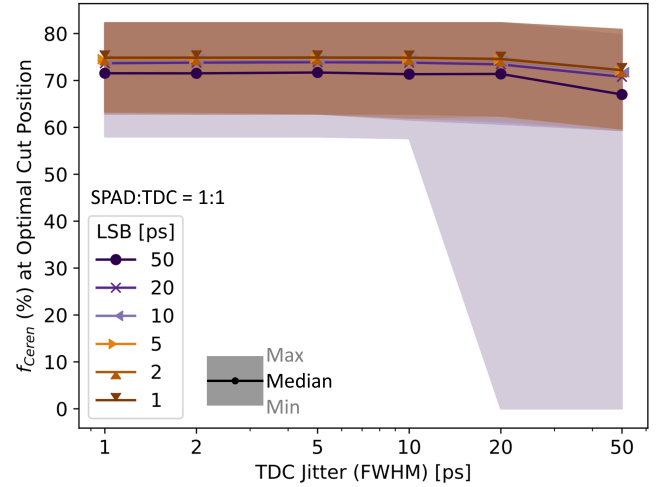


Fig. 4. Cerenkov separation (as  $f_{\text{Ceren}}$ ) of 96 photosensors vs. different TDC specifications with the optimal cut position for each sensor. Dots and lines depict medians while shaded areas show min and max values of 96 sensors.

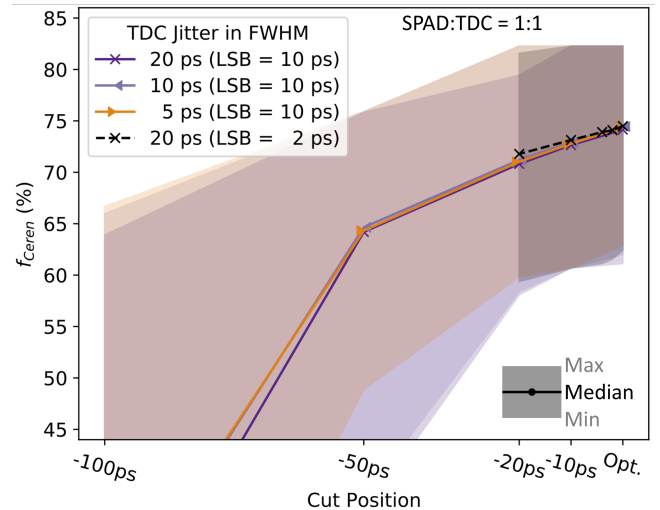


Fig. 5. Cerenkov separation (as  $f_{\text{Ceren}}$ ) vs. different cut positions. Optimal cut positions differ with sensors, and cut positions meeting cut conditions (\*) all have smaller timestamps than the optimal. Thus, x-axis displays other cuts relatively to the left of the optimal. Dots and lines depict medians while shaded areas show min and max values of 96 sensors.

In addition to the optimal cut position used in Fig. 4, we also studied the impact of different cut positions on the separation quality. Fig. 5 shows Cerenkov separation (as  $f_{\text{Ceren}}$ ) vs. different cut positions at four selected configurations. Within a 50 ps margin to the left of the optimal, at the same cut position, reducing jitter from 20 ps to 5 ps has minimal impact on separation performance. For the evaluated jitter values, within a 20 ps margin to the left of the optimal, the median  $f_{\text{Ceren}}$  of 96 sensors drops less than 4%. More to the left of the 50 ps margin, the Cerenkov separation drops significantly. From Fig. 5, it also suggests that for jitter  $\leq 20$  ps & LSB  $\leq 10$  ps, the 20 ps left margin gives at least 3 positions meeting cut conditions (\*) for all 96 sensors.

Therefore, to ensure time-based separation performance: 1) LSB  $\leq 10$  ps for sufficient cut positions, 2) cut positions within a 20 ps margin to the left of optimal position for approx.

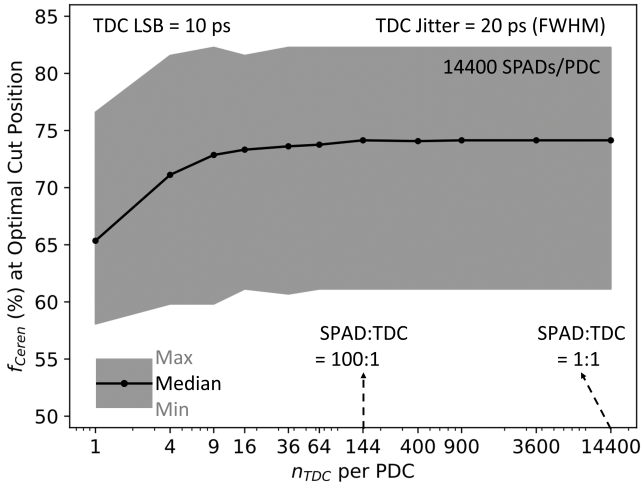


Fig. 6. Cerenkov separation (as  $f_{\text{Ceren}}$ ) of 96 photosensors vs.  $n_{\text{TDC}}$  per PDC with the optimal cut position for each sensor. Each SPAD-TDC group records the timing of the first arrival hit per event. Dots and lines depict medians while shaded areas show min and max values of 96 sensors.

70% Cerenkov separation, and 3) jitter  $\leq 20$  ps for efficient separation.

### B. SPAD:TDC Sharing Ratio

To evaluate how the SPAD:TDC sharing ratio affect the separation quality, we used the 20 ps jitter & 10 ps LSB configuration. The SPAD array has  $120 \times 120$  cells of  $50 \mu\text{m} \times 50 \mu\text{m}$ , thus 14400 SPADs per PDC. Each group of  $n \times n$  SPADs is considered to share a TDC, with  $n$  ranging from 1 to 120. Each SPAD-TDC group records the timing of only the first hit arrived per event.

Fig. 6 shows the Cerenkov separation (as  $f_{\text{Ceren}}$  detected at optimal cut positions) vs. the number of TDCs ( $n_{\text{TDC}}$ ). From this figure, with only 4 TDCs / 14400 SPADs (i.e., SPAD:TDC = 3600:1), the median  $f_{\text{Ceren}}$  is still 71%. The reason is that Cerenkov hits are rare and usually the first hit in events. Scintillation photons, mainly arriving later, experience pileup-related losses. Thus, it is possible to separate Cerenkov and scintillation with very few TDCs.

Fig. 7 shows the margin of positions meeting cut conditions (\*) around the optimal setting vs. the  $n_{\text{TDC}}$ . In the extreme case of 1 TDC / 14400 SPADs, all sensors still have a margin of at least 3 positions meeting cut conditions (\*), i.e. a margin of 20 ps. Based on LoLX Gen1 simulation photon time profile, the SPAD:TDC sharing ratio barely affects the detected  $n_{\text{Ceren}}$ . Thus, the  $n_{\text{TDC}}$  should be decided from each experiment's requirements, e.g. more TDCs to have more scintillation timestamps for photon counting, or fewer TDCs for waveform processing.

The results presented in this work are for the  $\beta$  source at the center of the LXe case. For different source positions, we expect a shift in the optimal cut position of each PDC corresponding to how close the PDC is to the interaction point. The performance of the time-based Cerenkov-scintillation separation may not degrade significantly as long as the prompt arrival of Cerenkov photons is maintained. For precise evaluation,

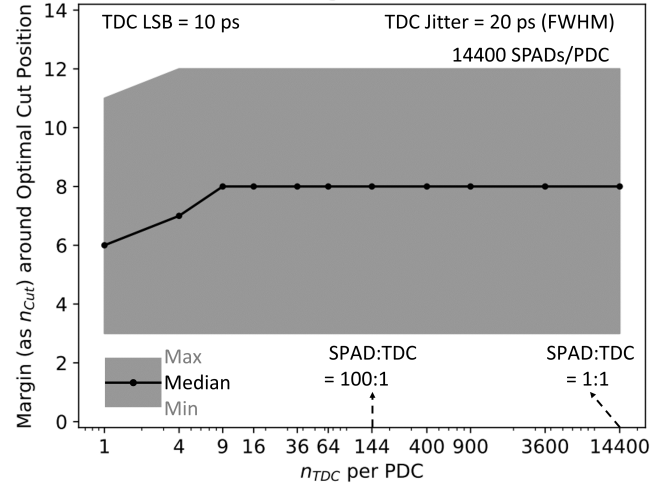


Fig. 7. Margin of positions meeting cut conditions (\*) around the optimal vs.  $n_{\text{TDC}}$  per PDC. The margin is to the left of the optimal (smaller timestamp direction). Dots and lines depict medians while shaded areas show min and max values of 96 sensors.

it is necessary to perform calibration for different interaction positions in future studies of LoLX.

## IV. SUMMARY & CONCLUSIONS

In this work, we used a PDC simulator, whose input is the light information from the LoLX simulation model, to study the effect of TDC parameters on the time-based Cerenkov separation's performance. This study aims to open specification margins for the ongoing development of LoLX PDCs, which, in the future, will replace current SiPMs used in LoLX.

TDC jitter and LSB results show that the time-based separation improves the Cerenkov detection on average from 54% (optical filters) to 71% (with 100% PDE). This 71% is indeed limited by the photon time profile of the LoLX simulation, which further indicates the effectiveness of the time-based separation. A configuration of 20 ps jitter & 10 ps LSB is enough to give a cut margin of at least 3 positions (20 ps to the left of the optimal) for all 96 sensors with an average of 70% separation. With the LoLX Gen1 simulation photon time profile, the SPAD:TDC sharing ratio results show that most  $n_{\text{Ceren}}$  can be detected with a few TDCs, e.g., 71%  $n_{\text{Ceren}}$  using 4 TDCs per PDC. Thus, the  $n_{\text{TDC}}$  should be decided from each experiment's timing requirements, e.g. photon counting or waveform processing.

The above findings offer a specification outline, specifically on TDC jitter and LSB, to speed up LoLX PDC development. Once these PDCs are ready, LoLX will be used to experimentally verify these simulations.

### ACKNOWLEDGMENT

The authors thank Julien Roy-Sabourin and David Paré for their help on matching LoLX simulation output with DSAS input. The authors also thank Gabriel Bélanger, Julien Rossignol, Xavier Groleau, and Audrey Corbeil Therrien for their help on using the DSAS package.

## REFERENCES

- [1] G. Adhikari *et al.*, “nEXO: neutrinoless double beta decay search beyond  $10^{28}$  year half-life sensitivity,” *Journal of Physics G: Nuclear and Particle Physics*, vol. 49, no. 1, p. 015104, 2021.
- [2] L. Galli *et al.*, “Looking for Cherenkov light in liquid xenon with LoLX,” *Nuclear Instruments and Methods in Physics Research Section A: Accelerators, Spectrometers, Detectors and Associated Equipment*, vol. 1047, p. 167876, 2023.
- [3] J. P. Brodsky *et al.*, “Background discrimination for neutrinoless double beta decay in liquid xenon using cherenkov light,” *Nucl. Instrum. Methods Phys. Res. A*, vol. 922, pp. 76–83, 2019.
- [4] S. Gundacker *et al.*, “Measurement of intrinsic rise times for various L(Y)SO and LuAG scintillators with a general study of prompt photons to achieve 10 ps in TOF-PET,” *Phys. Med. Biol.*, vol. 61, no. 7, pp. 2802–2837, 2016.
- [5] P. Lecoq *et al.*, “Roadmap toward the 10 ps time-of-flight PET challenge,” *Phys. Med. Biol.*, vol. 65, no. 21, p. 21RM01, 2020.
- [6] J.-F. Pratte *et al.*, “3D Photon-To-Digital Converter for Radiation Instrumentation: Motivation and Future Works,” *Sensors*, vol. 21, no. 2, 2021.
- [7] F. Nolet *et al.*, “A 2D Proof of Principle Towards a 3D Digital SiPM in HV CMOS With Low Output Capacitance,” *IEEE Trans. Nucl. Sci.*, vol. 63, no. 4, pp. 2293–2299, 2016.
- [8] A. Corbeil Therrien *et al.*, “Modeling of Single Photon Avalanche Diode Array Detectors for PET Applications,” *IEEE Trans. Nucl. Sci.*, vol. 61, no. 1, pp. 14–22, 2014.
- [9] G. Gallina *et al.*, “Characterization of the Hamamatsu VUV4 MPPCs for nEXO,” *Nuclear Instruments and Methods in Physics Research Section A: Accelerators, Spectrometers, Detectors and Associated Equipment*, vol. 940, pp. 371–379, 2019.
- [10] J. Allison *et al.*, “Recent developments in Geant4,” *Nuclear instruments and methods in physics research section A: Accelerators, Spectrometers, Detectors and Associated Equipment*, vol. 835, pp. 186–225, 2016.
- [11] E. Grace *et al.*, “Index of refraction, Rayleigh scattering length, and Sellmeier coefficients in solid and liquid argon and xenon,” *Nuclear Instruments and Methods in Physics Research Section A: Accelerators, Spectrometers, Detectors and Associated Equipment*, vol. 867, pp. 204–208, 2017.